Fluid Phase Equilibria 564 (2023) 113596

Contents lists available at ScienceDirect

Fluid Phase Equilibria

journal homepage: www.journals.elsevier.com/fluid-phase-equilibria

The monotonicity behavior of density profiles at vapor-liquid interfaces of mixtures

Simon Stephan *, Harry Cárdenas, Andrés Mejía, Erich A. Müller

Department of Chemical Engineering, Sargent Centre for Process Systems Engineering, Imperial College London, South Kensington Campus, London SW7 2AZ, United Kingdom

ARTICLE INFO

Keywords:
Vapor-liquid interface
Adsorption
Enrichment
Surface activity
Molecular simulation
Density gradient theory

ABSTRACT

In their seminal monograph 'Molecular Theory of Capillarity', *Rowlinson and Widom* describe different possible shapes of density profiles at the vapor-liquid interface of mixtures. They postulated that in some instances, density profiles could possibly be non-monotonic, exhibiting either a maximum and/or a minimum. This contribution revisits this statement in the light of four decades of posterior research. We summarize the distinct morphologies at the vapor-liquid interface suggested in the literature recognizing that the condition of a single minimum in the profile has not yet been reported. Interfacial density profiles with a single maximum as well as fully monotonic density profiles have been observed and reported extensively. The case of a simultaneous maximum and minimum is more controversial, as it has only been predicted using theoretical approaches such as density gradient theory (DGT). This ambiguity is further investigated in this work using the example of the vapor-liquid interface of cyclohexane + butanol. Both DGT in combination with several distinct equations of state and molecular dynamics simulations are used. The results from the two methods are found to be contradictory: while the DGT results predict a maximum/minimum structure, the computer experiment results indicate only a single maximum in the density profiles. This work thereby emphasizes that results from DGT for highly non-ideal mixtures should not be taken for granted.

1. Introduction

The reliable prediction and modeling of interfacial properties of mixtures is critical for the design of chemical, biological, and physical processes. Unfortunately, the molecular structure of fluid interfaces is challenging to probe using experimental methods due to the dynamical nature of the interface. The rapid thermal fluctuations at fluid interfaces and sharp density gradients occurring over the length of nanometers conspire against the experimental efforts to characterize the interfacial region. However, density and pressure profiles can be predicted by molecular modeling and simulation, namely molecular simulations using classical force field models [1–3] or theoretical methods such as density gradient theory (DGT) and density functional theory (DFT) [4–7] in conjunction with molecular-based free energy models [8–10] or structure based models (for example the Born-Green-Yvon approach (BGY) [7,11–13]). While molecular simulations can be applied in a strictly predictive manner in many cases and are therefore usually considered as reference, DGT and DFT usually require to some extent the parametrization of substance-specific model parameters. In spite that, both DGT and DFT are usually parameterized using macroscopic VLE property data, nanoscopic interfacial properties such as the density profiles are predicted by the theories.

Density profiles of vapor-liquid interfaces of mixtures may exhibit a non-monotonic behavior – also at equilibrium states, when the free energy is minimized. The monotonicity behavior of vapor-liquid interfaces of mixtures is of particular interest as non-monotonic density profiles are suspected to influence the mass transfer across interfaces [14–24]. The inference of the general shapes of the vapor-liquid density profiles is the starting point of all theoretical studies on interfacial properties [19,20,25–29]. Yet, no generally accepted framework has been established on the possible structures that can be expected at vapor-liquid interfaces, i.e. their topology. In their pioneering monograph *Rowlinson and Widom* [5] postulated the possibility for a maximum in the interfacial density profile as well as the possibility for a minimum in an interfacial density profile, which is continually recapitulated [30–32]. This work challenges this picture by reviewing which cases of interfacial structure have to date been confirmed and which are still disputable. It is pointed out that a minimum in interfacial density

* Corresponding author.
E-mail addresses: S.Stephan@imperial.ac.uk, simon.stephan@mv.uni-kl.de (S. Stephan).

https://doi.org/10.1016/j.fluid.2022.113596
Received 16 May 2022; Received in revised form 17 August 2022; Accepted 1 September 2022
Available online 13 September 2022
0378-3812/© 2022 The Author(s). Published by Elsevier B.V. This is an open access article under the CC BY license (http://creativecommons.org/licenses/by/4.0/).

profiles has only been reported in the literature in conjunction with a maximum [33–37] – so far to be considered a special and disputed case. An exemplary case (the mixture cyclohexane + n-butanol) is discussed in detail here using both molecular dynamics (MD) simulations and DGT. It is shown that the results from the two independent methods are contradictory: the density profiles obtained from molecular simulations yield a single maximum, whereas DGT predicts a maximum/minimum structure.

This work is outlined as follows: the current status on the knowledge of vapor-liquid density profiles of mixtures is discussed regarding what types of structures are generally possible and what structures have so far been observed. We propose a classification scheme, highlighting uncovered ambiguities in the literature. In the second section, we provide definitions of the interfacial properties used to quantify interfacial excess and discuss benefits, drawbacks, and pitfalls of different observables (which have at times caused confusion in the literature regarding the monotonicity behavior). The third section presents and discusses the interfacial properties results for the mixture cyclohexane + n-butanol from MD and DGT.

This work is limited to vapor-liquid interfaces of binary mixtures of molecular fluids. Interfaces of ionic liquids, surfactants, polymers, electrolyte solutions, and multi-component mixtures as well as liquid-liquid interfaces are not covered.

2. Structure of vapor-liquid interfaces

For vapor-liquid interfaces, two types of phenomena causing a non-monotonicity in density profiles can be generally distinguished: (1) the so-called surface activity featuring a single maximum or minimum or a combined maximum/minimum structure and (2) an oscillatory layering structure (OLS). Fig. 1 schematically shows these interfacial structures: Fig. 1(a)-(d) depict different types of surface activity and Fig. 1(e) the OLS. It should be noted that the classification scheme proposed in Fig. 1 is designed for vapor-liquid interfaces, i.e. liquid-liquid and dense fluid-fluid interfaces as well as fluid interfaces at three-phase equilibria may exhibit additional features [21,38–40].

The phenomenon of a single extremum (cf. Fig. 1a-d) is intimately linked to the phase behavior of a mixture [27,38,41]. This type of non-monotonicity is usually referred to as *enrichment* or *surface activity*. It can only exist at interfaces of mixtures. The oscillatory layering structure on the other hand is a purely structural phenomenon consisting of multiple extrema in density profiles (cf. Fig. 1(e)) with decaying amplitude towards the bulk liquid phase. It can occur at both pure substance and mixture vapor-liquid interfaces [16,33,42–45]. The vapor bulk phase of a vapor-liquid interface acts as an external field causing a layering of particles in the liquid phase with respect to the surface – similar to the adsorption phenomenon at solid-fluid interfaces. The OLS can be considered as the 'ending' of the radial distribution function of the liquid phase at the interface. The density decay from the liquid surface into the liquid bulk phase can occur with exponentially damped oscillations or be a monotonic decay – in accordance with the crossover between the oscillatory and monotonic decay of correlation functions in the bulk fluid. Hence, the occurrence and magnitude of an OLS depends on the temperature and pressure. The OLS is usually prominent at low temperatures, where the interface is thin and thermal fluctuations are only faint. The OLS can be captured by DFT, molecular simulations, and also BGY models [13,42], but is precluded in DGT [42,46] due to the underlying assumptions in the theory. Moreover, the OLS sampled from molecular simulations are strongly affected by surface wave fluctuations [42,47], which decreases the amplitude of the layering structure.

The OLS is a structural phenomenon affecting the entire liquid phase, i.e. all components, whereas the surface activity is usually found to only affect the low-boiling component in binary mixtures. The peak height of the surface activity is often on the order of magnitude of the density difference of the bulk phases. The peak height of the OLS is usually significantly smaller (but strongly depends on the method) than that of

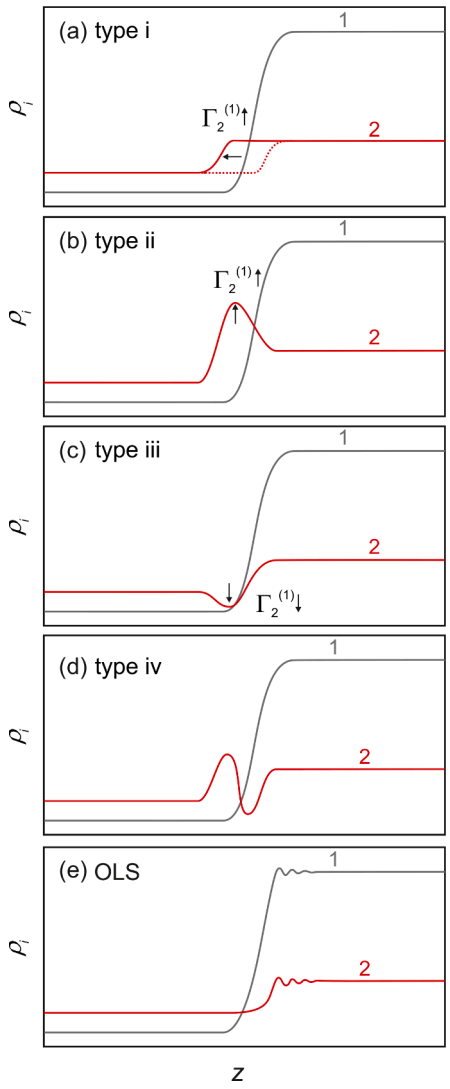


Fig. 1. Schemes of possible and postulated morphologies at vapor-liquid interfaces of a binary mixture: (a)-(d) show different types of surface activity; (e) shows an oscillatory layering structure (OLS). The high-boiling component 1 is depicted in gray and the low-boiling component 2 in red.

the surface activity, cf. Fig. 1. The surface activity non-monotonicity is usually located central at a vapor-liquid interface, i.e. it can not be unambiguously assigned to either the liquid or the vapor side of the interface and is an inherent part of the interphase. The OLS on the other hand occurs on the liquid side of the interface. In general, the two non-monotonicity morphologies may be present simultaneously causing the two structural phenomena to be superimposing each other, cf. Refs. [16,33,48].

When discussing the surface activity, four main types of structures could be postulated in general, cf. Fig. 1(a)-(d). They are labeled here type i-iv. For all four types, the high-boiling component density usually exhibits a monotonic transition between the two bulk phases [41]. In the case of azeotropic mixtures, the high-boiling component changes at the azeotropic point, which also causes a switchover in the density profile monotonicity behavior between the two components [40,49].

Depending on the monotonicity type, the low-boiling component may exhibit a monotonic or non-monotonic transition between the bulk phases, cf. Fig. 1(a)-(d). The surface activity monotonicity type is known to be directly linked to the phase behavior of the mixture [15,27,38,41,50]. For type i behavior, the low-boiling component density exhibits a monotonic transition between the bulk phases. This type of structural

behavior is often found and has been predicted by both theory (DGT or DFT) and computer experiment [41,51]. Both, ideal mixtures and high-boiling azeotropic mixtures are usually found to be of type i [15,40,41,41,50,51]. In the case of type ii behavior, the low-boiling component density exhibits a single distinct maximum. This structure type has been frequently confirmed in the literature by both theory and computer experiments [41]. Type ii is often observed for low-boiling azeotropic mixtures and mixtures with a supercritical component [20,40,49,50,52,53].

While both type i and type ii behavior have been observed multiple times in the literature [41], type iii interfacial behavior has, to the best of our knowledge, not yet been predicted by either computer simulations or a theory. This is intriguing since this type has been postulated by *Rowlinson and Widom* [5] and since then endorsed several times, e.g. Refs. [30–32]. Yet, type iii behavior presently remains unconfirmed. For type iv (a maximum followed by a minimum – upon approaching the liquid phase), theoretical predictions are available [33–37], but no computer experiment data have confirmed these results yet. Most of these results for type iv behavior also show an enrichment of the high-boiling components' density profile, i.e. a single maximum. In general, type iv may also consist of a minimum followed by a maximum, but such structure has to the best of our knowledge not yet been observed. Most authors reporting type iv results raise doubts of the physical soundness of these predictions [34,36,37]. The literature reporting type iv behavior is analyzed in detail in the following.

Mejía et al. report results [35] for alkane + alcohol mixtures with type iv interfacial behavior using DGT with the HR-SAFT EOS. *Camacho Vergara* et al. report DFT results [33] for mixtures of alkane + alcohol (e.g. n-hexane + ethanol) showing some features of a type iv behavior, but the presence of strong OLS in the DFT results impede a clear identification of the monotonicity type; e.g. they are consistent with a type ii with superimposed OLS (cf. Fig. 1).

Mairhofer and Gross [34] report results for several alkane + alcohol mixtures with type iv behavior. *Mairhofer and Gross* used DFT and DGT (both the classical reference density method and the stabilized DGT method) for their calculations in conjunction with the PCP-SAFT free energy model. In all studied cases both DGT methods predict type iv behavior – in contrast to the DFT, which predicts type ii behavior [34]. They address these differences to shortcomings regarding large gradients in the DGT, i.e. suggest the former results to be unphysical.

Cornelisse [36] also reports results for alkane + alcohol mixtures using DGT in conjunction with the Peng-Robinson EOS and the APACT EOS. The results from both EOS exhibit type iv behavior. *Cornelisse* implicitly suggests that this interfacial structure type is unrealistic, especially due to the large gradients between the maximum and the minimum of the density profile of the low-boiling component. In addition, he reports convergence issues for the case of the classical geometric mixing of cross-influence parameter. By introducing an additional parameter β_{ij}, those convergence problems are reported to be circumvented, which also changes the monotonicity behavior at some state points from type iv to type ii.

Both *Mairhofer and Gross* [34] and *Cornelisse* [36] state that introducing an additional β_{ij} parameter for the DGT cross-influence parameter $\kappa_{ij} = \beta_{ij}(\kappa_{ii}\kappa_{jj})^{1/2}$, leads to a reduction of the maximum/ minimum structure and the extreme gradients. It should however be noted that no physical justification of this β_{ij} parameter has yet been proposed in the literature to the best of our knowledge.

Liang et al. [37] report results for an alkane + alcohol mixture using DGT in conjunction with the simplified PC-SAFT EOS and the CPA EOS. They find type iv behavior, but suggest that the results are unrealistic due to the large density gradients at the interface [37].

In summary, the available type iv behavior results are predicted by DGT in conjunction with different EOS (except those of Ref. [33], which are probably type ii with strong OLS). Most of these results show very large (almost infinite) density gradients $\frac{d\rho_i}{dz}$ at the interface between the maximum and the minimum. Hence, it remains questionable if the density (square) gradient theory approximations are valid for these systems, i.e. low density gradients compared to the repulsive interaction range of the particles are a requirement in DGT [5].

3. Observables for vapor-liquid interfacial properties

The surface excess at vapor-liquid interfaces can in general be characterized by different observables. Here, 'surface excess' refers to deviations of the local composition in the interphase from the bulk phase compositions in a broad sense. Frequently used descriptors are the relative adsorption Γ [20,43] and the enrichment E [41,54]. The enrichment, E, quantifies the non-monotonicity of density profiles using the relative peak height computed as

$$E_i = \frac{\max(\rho_i(z))}{\max(\rho_i', \rho_i'')} \tag{1}$$

where $\rho_i(z)$ is the number density profile of component i across the vapor-liquid interface, z indicates the direction normal to a (nanoscopically) planar interface, and ρ_i' and ρ_i'' indicate the saturated liquid and vapor density, respectively. Evidently, this quantity can only be used in a meaningful way to characterize type i and type ii interfaces, cf. Fig. 1, whereas the relative adsorption Γ (defined below) can be used to characterize all types i-iv. The behavior of the enrichment E_i at type i and type ii interfaces has been reviewed recently in Ref. [41]. Thereby, a database with more than 2,000 entries is available for type i and ii behavior [41]. It was found, that the enrichment can be correlated using a simple and universal expression with the boiling behavior, i.e. the partition coefficient of a mixture. In general, strong enrichment is favored by low temperatures and low concentrations of the low-boiling component [41].

The monotonicity behavior of density profiles is often characterized by the *surface activity*, which is a quality (not quantity) defined according to the sign of the second derivative at an extremum [31,32], i.e. a maximum in a density profile (type ii) is considered 'positive surface activity' and a minimum (type iii) as 'negative surface activity', and a monotonous density profile (type i) as 'no surface activity'. In this context, type iv may be considered as 'ambivalent surface activity'. Furthermore, the surface excess can be characterized according to visual impressions from MD or MC simulation snapshots. However, these impressions can be misleading, since several quantities and phenomena are often superimposed.

The relative adsorption Γ can be used more rigorously than the 'surface activity' to quantify the surface excess. It quantifies the number of adsorbed molecules per unit area at the interface. In contrast to the enrichment and the surface activity, the relative adsorption is an integral measure for the interfacial composition. Hence, the relative adsorption does not quantify the monotonicity behavior of the density profiles (which is at times mistakenly supposed). However, the relative adsorption is influenced by the monotonicity behavior of the density profiles. The picture of the 'adsorption' being an integral measure for the interphase composition is prestressed in Gibbsian thermodynamics, which relates the integral interphase composition to thermodynamic potentials [5,55,56]. The Gibbs adsorption equation establishes a direct link between macroscopic observables and the (nanoscopic) relative adsorption at the interface: it relates the relative adsorption $\Gamma_i^{(j)}$ (adsorption of a component i with respect to a component j) to the dependency of the surface tension on the chemical potential [55]. The relative adsorption $\Gamma_i^{(j)}$ is thereby defined as

$$\Gamma_i^{(j)} = -\left(\frac{\partial \gamma}{\partial \mu_i}\right)_T, \tag{2}$$

where γ is the surface tension and μ_i is the chemical potential of component i in the equilibrated phases. Accordingly, using the term

'adsorption' to characterize the non-monotonicity behavior of density profiles is in general misleading. The relative adsorption $\Gamma_i^{(j)}$ can be determined experimentally (indirectly) from surface tension data in combination with a thermodynamic model for the chemical potentials – following Eq. (2).

As suggested above, the relative adsorption $\Gamma_i^{(j)}$ can be calculated from macroscopic properties or the nanoscopic density profiles $\rho_i(z)$ [57]. The nanoscopic definition for the relative adsorption is computed as an integral measure from the density profiles $\rho_i(z)$. Thereby, the relative adsorption $\Gamma_i^{(j)}$ can be obtained using a symmetric interface segregation [20,43]

$$\Gamma_i^{(j)} = -\left(\rho_i' - \rho_i''\right) \int_{-\infty}^{\infty} \left[\frac{\rho_j(z) - \rho_j'}{\rho_j' - \rho_j''} - \frac{\rho_i(z) - \rho_i'}{\rho_i' - \rho_i''} \right] \mathrm{d}z. \tag{3}$$

Results for the relative adsorption computed from the macroscopic route (Eq. 2) and the nanoscopic route (Eq. 3) are usually found to be in good agreement [19,31,32,43,52,58–66]. This suggests that the predicted density profiles (including an eventually present non-monotonicity) correspond to physical observables. Nevertheless, the monotonicity behavior of the density profiles (cf. Fig. 1) predicted from theory and molecular simulations including the enrichment E_2 has not yet been experimentally confirmed. We note in passing that the OLS will usually have no significant contribution to the relative adsorption.

For a binary mixture, a (positive) adsorption of a component *i* will in general be accompanied by a desorption (negative adsorption) of component *j* and vice versa [15,60]. The relative adsorption is related to the monotonicity behavior of the density profiles, but not in a unique way. Relative adsorption (positive or negative) according Eq. (3) can be caused by two mechanisms: a relative shift of the two component density profiles and a non-monotonicity of a profile. For type i behavior, such a shift is schematically depicted in Fig. 1(a). A relative shift of density profiles can in general also appear for the other types and cause relative adsorption of a component, cf. Refs. [15,40,50,52]. The shift is not depicted for type ii-iv to avoid visual clutter.

For positive surface activity, an increasing peak height of the density profile for component *i* will in general increase the relative adsorption $\Gamma_i^{(j)}$ (cf. Fig. 1b). For negative surface activity, an increasing depletion depth of the density profile of component *i* would in general decrease the relative adsorption $\Gamma_i^{(j)}$ (cf. Fig. 1c). For an ambivalent surface activity (cf. Fig. 1d), the impact of a relative shift of the density profiles and the peak hights can have different effects on the relative adsorption – depending on the details of the interfacial structure.

Hence, depending on the two features of the density profiles (relative shift and monotonicity), positive, negative, or zero relative adsorption of a component *i* can be observed for different monotonicity types (cf. Fig. 1): type i behavior (no surface activity; cf. Fig. 1) with positive relative adsorption of the low-boiling component has been observed for ideal mixtures (in the sense of Raoult's law) [15,38,51]. Furthermore, type i behavior with either positive, negative or zero relative adsorption (depending on temperature and composition) of a low-boiling component has been observed for high-boiling azeotropic mixtures [15,40,51]. Type ii behavior (positive surface activity) with positive relative adsorption of the low-boiling component at all state points is frequently observed in mixtures with a supercritical component [19,31,32,38,52,54,59,61–64,67–70] and mixtures with wide-boiling phase behavior (both components being subcritical) [60,71,72]. Also, type ii behavior mixtures with positive, negative or zero relative adsorption of a low-boiling component (depending on temperature and composition) has been observed [15,20,40,49,51,73], e.g. for low-boiling azeotropic mixtures.

4. Interfacial properties of the mixture cyclohexane + n-butanol

As an exemplaric system of the type alkane + alcohol, which could potentially exhibit a type iv behavior, the mixture cyclohexane + n-butanol was studied in this work using density gradient theory (DGT) in combination with different equations of state (EOS) as well as molecular dynamics simulation. For the molecular simulations, classical direct VLE simulations in the NVT ensemble were performed with 6 000 molecules using the pcff+ all atom force field [74,75] and the LAMMPS code [76]. Equilibration was carried out for 5 ns and the production time was 50 ns. The time step was 1 fs. Further simulation details are given in the Supplementary Material. The DGT calculations were performed using the PC-SAFT [77], CPA [78], and SAFT-VR Mie EOS [79]; Pure component model parameters were taken from Refs. [77–82] We employed the stabilized density gradient theory (sDGT) method proposed by *Mu* et al. [83]. Here, the interfacial property results obtained from DGT for the mixture are pure predictions since the influence parameter was only fitted for the pure components and the geometric combination rule was applied for computing the mixture influence parameter. [15]

Fig. 2 shows the isothermal $p-x$ phase diagram at 303.15 K computed by the three EOS. The binary interaction parameter of the combination rule was adjusted to experimental phase equilibrium data at 308.15 K. The mixture cyclohexane + butanol exhibits a low-boiling azeotrope at a mole fraction of cyclohexane of approximately $x_{\mathrm{cyc}} = 0.95\,\mathrm{mol\,mol^{-1}}$, i.e. in the vicinity of pure cyclohexane (which is captured by all three studied EOS). The two-phase region between pure butanol and the azeotropic point is particularly wide-boiling. While the phase equilibrium pressure of the force field significantly overestimates the experimental and EOS data (cf. Supplementary Material), the partition coefficient obtained from MD is in good agreement with that obtained from the EOS, cf. Supplementary Material for details.

Mixtures with low-boiling azeotropic behavior are mostly reported to exhibit an enrichment of the low-boiling component in the respective two-phase region [15,20,40,49,50], i.e. type ii behavior (cf. Fig. 1b). Fig. 3 shows the density profiles computed by DGT with the SAFT-VR Mie EOS at 303.15 K in the entire composition range. Evidently, DGT predicts a type iv interfacial behavior (ambivalent surface activity): the low-boiling component cyclohexane exhibits a combined maximum/minimum structure. Moreover, the high-boiling component butanol exhibits a maximum at the interface. The equivalent plots obtained using the CPA and PC-SAFT EOS are given in the Supplementary Material. They yield the same qualitative results, i.e. type iv behavior.

Fig. 3 reveals that, starting at low cyclohexane concentration, cyclohexane exhibits a strong enrichment at the interface and a shallow swale (depletion), while the butanol density profile exhibits a monotonous transition between the bulk phases. With increasing cyclohexane concentration, both the peak height and the swale depth of the cyclohexane profile increases. Also the butanol profiles start exhibiting a distinct maximum, even at low cyclohexane concentration $x'_{\mathrm{cyc}} \approx 0.1\,\mathrm{mol\,mol^{-1}}$.

In a wide composition range, the density profiles of both components

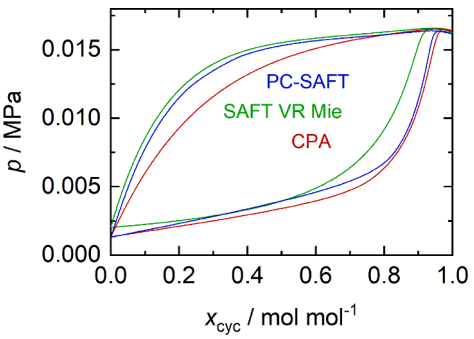


Fig. 2. $p-x$ phase diagram of the binary mixture of cyclohexane + butanol at 303.15 K. Results from the SAFT-VR Mie, PC-SAFT, and CPA EOS (color coded).

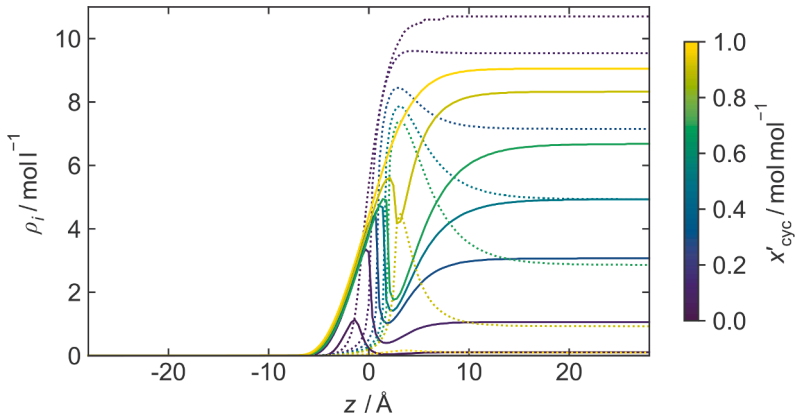


Fig. 3. Density profiles of the binary mixture of cyclohexane + butanol at 303.15 K. The liquid phase mole fraction of cyclohexane is color coded. Results from DGT + SAFT-VR Mie EOS. The dotted line indicates butanol; the solid line cyclohexane. The depicted concentrations are $x'_{cyc} = 0.01, 0.1, 0.3, 0.5, 0.7, 0.9, 0.99\,\mathrm{mol\,mol^{-1}}$.

exhibit extreme (almost infinite) gradients at the interface – especially the cyclohexane profiles between the maximum and the minimum. These gradients are problematic for the theory, as DGT is known to be only valid in the limit of small gradients. This type of stability problem for alkane + alcohol mixtures using DGT has also been reported in conjunction with several other EOS and critically discussed in the literature [34,36,37]. Also the CPA and PC-SAFT results (see Supplementary Material) show such extreme gradients. Only at infinite dilution in the vicinity of both pure components, the density profiles of both components exhibit moderate gradients, cf. Fig. 3.

Fig. 4 shows the DGT results obtained from the different molecular-based EOS at $x'_{cyc} = 0.5\,\mathrm{mol\,mol^{-1}}$. All DGT results predict type iv interfacial structure. *Mejía* et al. used the HR-SAFT EOS with DGT for the same mixture and state point and also found a type iv behavior. *Cornelisse* [36] studied the mixtures hexane + ethanol and hexane + propanol using the Peng-Robinson EOS and the APACT EOS with DGT also finding type iv behavior. *Mairhofer and Gross* [34] studied hexane + different alcohols using PCP-SAFT with DGT and also found type iv behavior. Hence, the maximum/minimum structure is probably not a result of a defect in a chosen EOS. However, it should be noted, that the results obtained from the CPA EOS exhibit more moderate gradients than the other EOS employed in this work. Moreover, the total density profiles predicted by the PC-SAFT and SAFT-VR Mie EOS exhibit a faint maximum, which is not found in the CPA results.

Three state points were studied by MD at 303.15 K: $x'_{cyc} \approx 0.25\,\mathrm{mol\,mol^{-1}}$, $x'_{cyc} \approx 0.5\,\mathrm{mol\,mol^{-1}}$, and $x'_{cyc} \approx 0.75\,\mathrm{mol\,mol^{-1}}$. The equilibrated density profiles obtained from molecular simulations for these conditions are shown in Fig. 5. The molecular simulation results show a type ii behavior, i.e. a single (faint) maximum in the density profiles of the low-boiling component cyclohexane at the interface. It is well known [84–86] that associating mixtures can exhibit micro-structuring in the bulk phases. This is also observed in the molecular simulation results from this work (see Supplementary Material). It is an open question, how this type of local micro-structure in the bulk phase affects interfacial properties. For the studied mixture, the interfacial structure predicted by the molecular simulation computer experiment (type ii) is considered a reference, supporting the inference that the DGT type iv predictions are misleading.

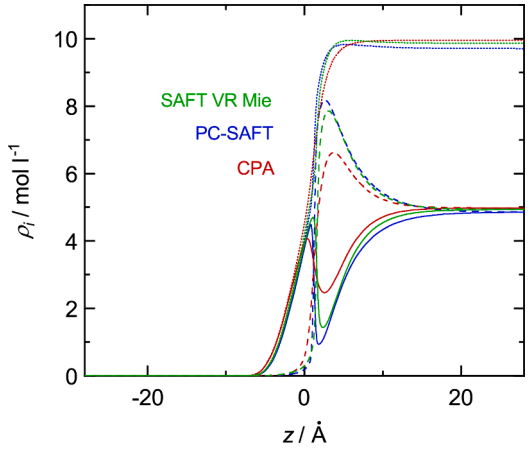


Fig. 4. Density profiles of the binary mixture of cyclohexane + butanol at 303.15 K and a liquid phase concentration of $x'_{cyc} = 0.5\,\mathrm{mol\,mol^{-1}}$. Results from DGT + different EOS (color coded). The dashed line indicates butanol, the solid line cyclohexane, and the dotted line the total density.

Fig. 6 shows the interfacial properties (surface tension, relative adsorption, and interfacial thickness) obtained from DGT using different EOS and MD. The pure component surface tension results are reported in the Supplementary Material. For the mixture results depicted in Fig. 6, the temperature was $T = 303.15$ K. The results from the three EOS are in qualitative agreement (for all three shown properties). Also the MD surface tension results show the same trend in the mixture, but the DGT results systematically underestimate the MD results.

Moreover, significant quantitative deviations among the three EOS results are observed for all three studied properties: the deviation among the three methods is about 10% for the surface tension, but the relative adsorption deviates up to a factor of four, and up to 50% for the interfacial thickness.

Starting at pure butanol, upon increasing the cyclohexane mole fraction in the liquid phase, the relative adsorption predicted by DGT is first positive (cyclohexane adsorbs at the interface), exhibits a zero crossing, and is then negative (cyclohexane desorbs at the interface). From the MD results shown in Fig. 5, it can be seen that the two component density profiles are shifted with respect to each other. Both the slight enrichment of cyclohexane, but in particular the density profile shift, contribute to a positive relative adsorption of cyclohexane, cf. Fig. 6. This is in conflict to the predictions from DGT, which yield a negative relative adsorption of cyclohexane at that condition (cf. Fig. 6). This behavior (enrichment of the low-boiling component accompanied by a density profile shift) has also been reported for a hexane + butanol mixture predicted by DFT by *Mairhofer and Gross* [34], whereas their DGT calculations also showed type ii behavior.

The concentration at which there is a minimum surface tension and zero relative adsorption is referred to as *aneotropic* point [87]. Low-boiling azeotropic mixtures often exhibit aneotropic behavior[15, 49,51,88]. Usually, the aneotropic point is found to be in good agreement with the azeotropic point [15,40,51,88]. However, for the binary mixture cyclohexane + butanol, DGT yields an aneotropic point at approximately $x'_{cyc} \approx 0.3\,\mathrm{mol\,mol^{-1}}$ (at 303.15 K), which is far off the

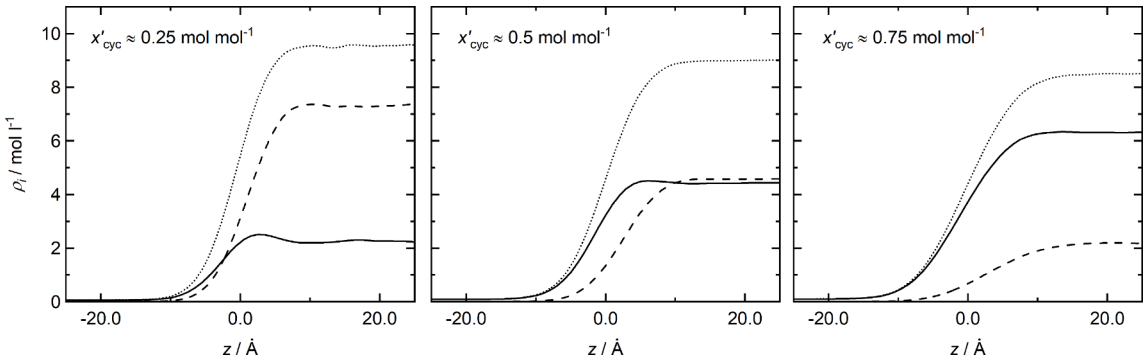


Fig. 5. Density profiles of the binary mixture cyclohexane + butanol at 303.15 K at three state points. Results from molecular dynamics simulations. The bulk phase concentrations and the equilibrium pressure are reported in the Supplementary Material. The dashed line indicates butanol, the solid line cyclohexane, and the dotted line the total density.

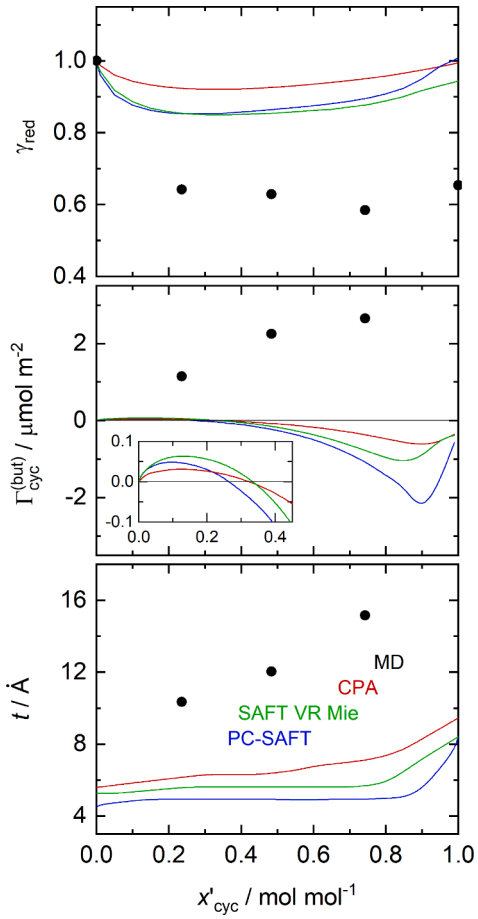


Fig. 6. Interfacial properties of the binary mixture cyclohexane + butanol at 303.15 K: surface tension (top), relative adsorption of cyclohexane (middle), and interfacial thickness (bottom) as a function of the liquid phase mole fraction of cyclohexane x'_{cyc}. Results from DGT (lines) in conjunction with different EOS (color coding is the same in all three plots) and MD (symbols). For the surface tension, the reduced values with respect to the pure component value of butanol $\gamma_{red} = \gamma/\gamma_{pure}$ are shown.

azeotropic composition at that temperature.

Experimental surface tension data for the mixture cyclohexane + butanol is scarce [89]. From that data[89], the aneotropic composition can not be reliably estimated. *Mairhofer and Gross* [34] studied the mixture n-hexane + ethanol (exhibiting a similar phase behavior as cycohexane + butanol) using DGT (and DFT) with the PCP-SAFT free energy model. For 298.15 K, DGT results of *Mairhofer and Gross*[34] also show an aneotropic point, which does not coincide with the azeotropic point at that temperature [34,37,89]. For the mixture n-hexane + ethanol, experimental surface tension data is available, which does not exhibit an aneotropic point (within the uncertainty of the data) [34,89] – on the contrary to the DGT predictions [34]. The DFT surface tension predictions are, on the other hand, in accordance with the experimentally observed behavior. Hence, it appears that even the qualitative surface tension results of the DGT are disputable.

The interfacial thickness (cf. Fig. 6–bottom) was computed using the 10-90% definition [90]. The interfacial thickness of the low-boiling pure component cyclohexane is larger than that of pure butanol at 303.15 K. With increasing cyclohexane concentration, DGT predicts a monotonous increase of the interfacial thickness. This is in agreement with the MD results. It is well known that MD results often show larger interfacial thickness due to surface fluctuations present in the dynamic method, which is also found in this work. The DGT results moreover predict a large plateau in a wide composition range. This plateau is a result of the extreme gradients of the density profiles at the interface. This is supported by the fact that the plateau is more pronounced in the SAFT-VR Mie and PC-SAFT results compared to the CPA results. The latter is found to exhibit more moderate gradients (see Supplementary Material for details).

5. Conclusions

Density profiles at vapor-liquid interfaces can exhibit complex structures. This work highlights and discusses ambiguities in this field. Two phenomena can produce a non-monotonicity of such profiles: multiple (decaying) oscillations on the liquid side of the interface and single distinct maxima or minima central at the interface. We introduce a classification scheme for the different morphology types that have so far been suggested in the literature: they are termed types i-iv. Results for type i behavior (monotonous density profiles) and type ii behavior (a single distinct maximum in a density profile) have been reported in the literature multiple times [41]. Type iii behavior (a single distinct minimum in a density profile) has been postulated in the literature [5], but not been confirmed by theoretical calculations or computer experiments yet. Singularly, type iv behavior has so far only been predicted by DGT [34–37].

An exemplaric potential type iv mixture was studied in detail in the present work using both density gradient theory and molecular simulations. We find that a combined maximum/ minimum structure is predicted by all employed equations of state using DGT. However, the MD results (which should be taken as reference) from this work seem to indicate that the DGT predictions (classical square gradient approximation) for type iv behavior are artificial. These contradicting results require further research in future work and would of course benefit from

being eventually resolved by experiments. For future work, a comprehensive comparison of molecular simulation results and predictions from theories (including both DGT and DFT) for highly non-ideal systems such as alkane + alcohol would be interesting.

A working hypothesis is, that a wide boiling phase behavior in combination with azeotropic behavior is related to the extreme gradients at the interface, which produce the maximum/ minimum structure. These extreme density gradients, however, conflict with the square gradient approximations made in classical DGT. Hence, the classical engineering DGT framework should be used with extra caution in such cases.

It remains an unresolved question if type iii and iv behavior are physically realizable.

CRediT authorship contribution statement

Simon Stephan: Conceptualization, Software, Investigation, Writing – original draft. **Harry Cárdenas:** Investigation. **Andrés Mejía:** Visualization, Validation. **Erich A. Müller:** Resources, Writing – review & editing.

Declaration of Competing Interest

The authors declare that they have no known competing financial interests or personal relationships that could have appeared to influence the work reported in this paper.

Acknowledgments

The author SiSt gratefully acknowledges funding of the present work by the DAAD (grant agreement No. 91774746). The authors are grateful to Benjamin Widom for fruitful discussions and the encouragement to reopen this topic.

Supplementary material

Supplementary material associated with this article can be found, in the online version, at 10.1016/j.fluid.2022.113596

References

[1] B.L. Eggimann, A.J. Sunnarborg, H.D. Stern, A.P. Bliss, J.I. Siepmann, An online parameter and property database for the TraPPE force field, Mol. Simul. 40 (1–3) (2014) 101–105, https://doi.org/10.1080/08927022.2013.842994.
[2] S. Stephan, M. Horsch, J. Vrabec, H. Hasse, MolMod - an open access database of force fields for molecular simulations of fluids, Mol. Simul. 45 (10) (2019) 806–814, https://doi.org/10.1080/08927022.2019.1601191.
[3] E.A. Müller, G. Jackson, Force-field parameters from the SAFT-γ equation of state for use in coarse-grained molecular simulations, Annual Review of Chemical and Biomolecular Engineering 5 (1) (2014) 405–427, https://doi.org/10.1146/annurev-chembioeng-061312-103314.
[4] R. Evans, Fundamentals of Inhomogeneous Fluids, Marcel Dekker, New York, 1992.
[5] J.S. Rowlinson, B. Widom, Molecular Theory of Capillarity, Dover Publications, New York, 1982.
[6] B. Carey. The Gradient Theory of Fluid Interfaces, University of Minnesota, Minneapolis, 1979. Ph.D. thesis.
[7] J. Fischer, U. Heinbuch, Relationship between free energy density functional, Born-Green-Yvon, and potential distribution approaches for inhomogeneous fluids 88(3) 1909–1913. 10.1063/1.454114.
[8] S. Stephan, J. Staubach, H. Hasse, Review and comparison of equations of state for the Lennard-Jones fluid, Fluid Phase Equilibr. 523 (2020) 112772, https://doi.org/10.1016/j.fluid.2020.112772.
[9] E.A. Müller, K.E. Gubbins, Molecular-based equations of state for associating fluids: A review of SAFT and related approaches, Ind. Eng. Chem. Res. 40 (10) (2001) 2193–2211, https://doi.org/10.1021/ie000773w.
[10] K.E. Gubbins, Perturbation theories of the thermodynamics of polar and associating liquids: A historical perspective, Fluid Phase Equilib. 416 (2016) 3–17, https://doi.org/10.1016/j.fluid.2015.12.043.
[11] J. Fischer, M. Methfessel, Born-Green-Yvon approach to the local densities of a fluid at interfaces, Phys. Rev. A 22 (1980) 2836–2843, https://doi.org/10.1103/PhysRevA.22.2836.
[12] M. Wendland, Liquid-liquid and liquid-vapour interfaces and wetting phenomena in the system methane-perfluoromethane calculated with the Born-Green-Yvon equation, Fluid Phase Equilib. 147 (1) (1998) 105–122, https://doi.org/10.1016/S0378-3812(98)00218-0.
[13] M. Wendland, Born-Green-Yvon results for the liquid-vapour interface of pure fluids and binary model mixtures, Fluid Phase Equilib. 141 (1) (1997) 25–43, https://doi.org/10.1016/S0378-3812(97)00212-4.
[14] S. Stephan, K. Langenbach, H. Hasse, Enrichment of components at vapour-liquid interfaces: A study by molecular simulation and density gradient theory, Chem. Engineer. Trans. 69 (2018) 295–300, https://doi.org/10.3303/CET1869050.
[15] S. Stephan, K. Langenbach, H. Hasse, Interfacial properties of binary Lennard-Jones mixtures by molecular simulations and density gradient theory, J. Chem. Phys. 150 (17) (2019) 174704, https://doi.org/10.1063/1.5093603.
[16] C. Klink, J. Gross, A density functional theory for vapor-liquid interfaces of mixtures using the perturbed-chain polar statistical associating fluid theory equation of state, Ind. Eng. Chem. Res. 53 (14) (2014) 6169, https://doi.org/10.1021/ie4029895.
[17] R. Nagl, P. Zimmermann, T. Zeiner, Interfacial mass transfer in water-toluene systems, J. Chem. Eng. Data 65 (2) (2020) 328–336, https://doi.org/10.1021/acs.jced.9b00672.
[18] R. Nagl, T. Zeiner, P. Zimmermann, Interfacial mass transfer in quaternary liquid-liquid systems, Chem. Eng. Process. - Process Intensification 171 (2022) 108501, https://doi.org/10.1016/j.cep.2021.108501.
[19] D.J. Lee, M.M. Telo da Gama, K.E. Gubbins, The vapour-liquid interface for a Lennard-Jones model of argon-krypton mixtures, Mol. Phys. 53 (5) (1984) 1113–1130, https://doi.org/10.1080/00268978400102891.
[20] M.M. Telo da Gama, R. Evans, The structure and surface tension of the liquid-vapour interface near the upper critical end point of a binary mixture of Lennard-Jones fluids I. the two phase region, Mol. Phys. 48 (2) (1983) 229–250, https://doi.org/10.1080/00268978300100181.
[21] J.M. Garrido, M.M. Piñeiro, A. Mejía, F.J. Blas, Understanding the interfacial behavior in isopycnic Lennard-Jones mixtures by computer simulations, Phys. Chem. Chem. Phys. 18 (2016) 1114–1124, https://doi.org/10.1039/C5CP06562C.
[22] S. Enders, H. Kahl, Interfacial properties of water + alcohol mixtures, Fluid Phase Equilib. 263 (2) (2008) 160–167, https://doi.org/10.1016/j.fluid.2007.10.006.
[23] B. Karlsson, R. Friedman, Dilution of whisky – the molecular perspective, Sci. Rep. 7 (6489) (2017) 1–9, https://doi.org/10.1038/s41598-017-06423-5.
[24] S. Stephan, D. Schaefer, K. Langenbach, H. Hasse, Mass transfer through vapour-liquid interfaces: a molecular dynamics simulation study, Mol. Phys. 119 (3) (2021) e1810798, https://doi.org/10.1080/00268976.2020.1810798.
[25] M.M. Telo da Gama, R. Evans, Theory of the liquid-vapour interface of a binary mixture of Lennard-Jones fluids, Mol. Phys. 41 (5) (1980) 1091–1112, https://doi.org/10.1080/00268978000103811.
[26] B.S. Carey, L.E. Scriven, H.T. Davis, Semiempirical theory of surface tension of binary systems, AIChE J. 26 (5) (1980) 705–711, https://doi.org/10.1002/aic.690260502.
[27] A.H. Falls, L.E. Scriven, H.T. Davis, Adsorption, structure, and stress in binary interfaces, J. Chem. Phys. 78 (12) (1983) 7300–7317, https://doi.org/10.1063/1.444720.
[28] M.M. Telo da Gama, R. Evans, The structure and surface tension of the liquid-vapour interface near the upper critical end point of a binary mixture of Lennard-Jones fluids II. the three phase region and the Cahn wetting transition, Mol. Phys. 48 (2) (1983) 251–266, https://doi.org/10.1080/00268978300100191.
[29] D.J. Lee, M.M. Telo da Gama, K.E. Gubbins, Adsorption and surface tension reduction at the vapor-liquid interface, J. Phys. Chem. 89 (8) (1985) 1514–1519, https://doi.org/10.1021/j100254a041.
[30] G. Alonso, G. Chaparro, M. Cartes, E.A. Müller, A. Mejía, Probing the interfacial behavior of type IIIa binary mixtures along the three-phase line employing molecular thermodynamics, Molecules 25 (7) (2020) 1499, https://doi.org/10.3390/molecules25071499.
[31] E.A. Müller, A. Mejía, Interfacial properties of selected binary mixtures containing n-alkanes, Fluid Phase Equilib. 282 (2) (2009) 68–81, https://doi.org/10.1016/j.fluid.2009.04.022.
[32] A. Mejía, M. Cartes, H. Segura, E.A. Müller, Use of equations of state and coarse grained simulations to complement experiments: Describing the interfacial properties of carbon dioxide + decane and carbon dioxide + eicosane mixtures, J. Chem. Eng. Data 59 (10) (2014) 2928, https://doi.org/10.1021/je5000764.
[33] E.L. Camacho Vergara, G.M. Kontogeorgis, X. Liang, On the study of the vapor-liquid interface of associating fluids with classical density functional theory, Fluid Phase Equilib. 522 (2020) 112744, https://doi.org/10.1016/j.fluid.2020.112744.
[34] J. Mairhofer, J. Gross, Modeling properties of the one-dimensional vapor-liquid interface: Application of classical density functional and density gradient theory, Fluid Phase Equilib. 458 (2018) 243–252, https://doi.org/10.1016/j.fluid.2017.11.032.
[35] A. Mejía, H. Segura, J. Wisniak, I. Polishuk, Association and molecular chain length effects on interfacial behavior, Phys. Chem. Liquids 44 (1) (2006) 45–59, https://doi.org/10.1080/00319100500303304.
[36] P.M. Cornelisse. The Square Gradient Theory Applied Simultaneous Modelling of Interfacial Tension and Phase Behaviour, Technische Universiteit Delft, 1997. Ph. D. thesis.
[37] X. Liang, M.L. Michelsen, G.M. Kontogeorgis, Pitfalls of using the geometric-mean combining rule in the density gradient theory, Fluid Phase Equilib. 415 (2016) 75–83, https://doi.org/10.1016/j.fluid.2016.01.047.
[38] S. Stephan, H. Hasse, Interfacial properties of binary mixtures of simple fluids and their relation to the phase diagram, Phys. Chem. Chem. Phys. 22 (22) (2020) 12544–12564, https://doi.org/10.1039/d0cp01411g.

[39] J.M. Garrido, H. Quinteros-Lama, J.M. Míguez, F.J. Blas, M.M. Piñeiro, On the physical insight into the barotropic effect in the interfacial behavior for the H_2O + Co_2 mixture 123(46) 28123–28130. 10.1021/acs.jpcc.9b07356.

[40] J. Staubach, S. Stephan, Interfacial properties of binary azeotropic mixtures of simple fluids: Molecular dynamics simulation and density gradient theory, J. Chem. Phys. 157 (2022) 124702, https://doi.org/10.1063/5.0100728.

[41] S. Stephan, H. Hasse, Enrichment at vapour-liquid interfaces of mixtures: Establishing a link between nanoscopic and macroscopic properties, Int. Rev. Phys. Chem. 39 (3) (2020) 319–349, https://doi.org/10.1080/0144235X.2020.1777705.

[42] S. Stephan, J. Liu, K. Langenbach, W.G. Chapman, H. Hasse, Vapor-liquid interface of the Lennard-Jones truncated and shifted fluid: Comparison of molecular simulation, density gradient theory, and density functional theory, J. Phys. Chem. C 122 (43) (2018) 24705–24715, https://doi.org/10.1021/acs.jpcc.8b06332.

[43] T. Wadewitz, J. Winkelmann, Density functional theory: Structure and interfacial properties of binary mixtures, Berichte der Bunsengesellschaft für physikalische Chemie 100 (11) (1996) 1825–1832, https://doi.org/10.1002/bbpc.19961001112.

[44] R. Evans, J.R. Henderson, D.C. Hoyle, A.O. Parry, Z.A. Sabeur, Asymptotic decay of liquid structure: Oscillatory liquid-vapour density profiles and the Fisher-Widom line, Mol. Phys. 80 (4) (1993) 755–775, https://doi.org/10.1080/00268979300102621.

[45] A.J. Archer, R. Evans, Binary Gaussian core model: Fluid-fluid phase separation and interfacial properties, Phys. Rev. E 64 (2001) 041501, https://doi.org/10.1103/PhysRevE.64.041501.

[46] R. Evans, Oscillatory behaviour of density profiles: Relevance for fluid interfacial phenomena, Berichte der Bunsengesellschaft für physikalische Chemie 98 (3) (1994) 345–352, https://doi.org/10.1002/bbpc.19940980312.

[47] M.R. Rahman, L. Shen, J.P. Ewen, D. Dini, E.R. Smith, The intrinsic fragility of the liquid-vapor interface: A stress network perspective, Langmuir 38(15) 4669–4679. 10.1021/acs.langmuir.2c00201.

[48] J. Winkelmann, The liquid-vapour interface of pure fluids and mixtures: Application of computer simulation and density functional theory, J. Phys. Condens. Matter 13 (21) (2001) 4739.

[49] E. Schäfer, G. Sadowski, S. Enders, Interfacial tension of binary mixtures exhibiting azeotropic behavior: Measurement and modeling with PCP-SAFT combined with density gradient theory, Fluid Phase Equilib. 362 (2014) 151, https://doi.org/10.1016/j.fluid.2013.09.042.

[50] S. Stephan, H. Hasse, Molecular interactions at vapor-liquid interfaces: Binary mixtures of simple fluids, Phys. Rev. E 101 (2020) 012802, https://doi.org/10.1103/PhysRevE.101.012802.

[51] S. Stephan, H. Hasse, Influence of dispersive long-range interactions on properties of vapour-liquid equilibria and interfaces of binary Lennard-Jones mixtures, Mol. Phys. 118 (9-10) (2020) e1699185, https://doi.org/10.1080/00268976.2019.1699185.

[52] S. Stephan, S. Becker, K. Langenbach, H. Hasse, Vapor-liquid interfacial properties of the binary system cyclohexane + CO_2: Experiment, molecular simulation and density gradient theory, Fluid Phase Equilibr. 518 (2020) 112583, https://doi.org/10.1016/j.fluid.2020.112583.

[53] B. González-Barramuño, E. Cea-Klapp, I. Polishuk, R.I. Canales, H. Quinteros-Lama, J.M. Garrido, Interfacial properties of fluorinated (f)-gases in azeotropic condition, J. Mol. Liq. 350 (2022) 118604, https://doi.org/10.1016/j.molliq.2022.118604.

[54] S. Becker, S. Werth, M. Horsch, K. Langenbach, H. Hasse, Interfacial tension and adsorption in the binary system ethanol and carbon dioxide: Experiments, molecular simulation and density gradient theory, Fluid Phase Equilib. 427 (2016) 476, https://doi.org/10.1016/j.fluid.2016.08.007.

[55] R. Defay, I. Prigogine, A. Bellmans, D.H. Everett, Surface Tension and Adsorption, Longmans, London, 1966.

[56] J.W. Gibbs, The Scientific Papers of J. W. Gibbs, Dover Publications, 1961.

[57] M.M. Telo da Gama, R. Evans, Surface segregation and surface tension at the liquid-vapour interface of a binary mixture of Lennard-Jones fluids, J. Chem. Soc., Faraday trans. 16 (1981) 45–58, https://doi.org/10.1039/FS9811600045.

[58] V.G. Baidakov, M.N. Khotienkova, Surface tension of methane-nitrogen solutions: 2. description in the framework of the van der Waals gradient theory, Fluid Phase Equilib. 425 (2016) 402–410, https://doi.org/10.1016/j.fluid.2016.06.038.

[59] T. Lafitte, B. Mendiboure, M.M. Piñeiro, D. Bessières, C. Miqueu, Interfacial properties of water/CO_2: A comprehensive description through a gradient theory SAFT-VR Mie approach, The Journal of Physical Chemistry B 114 (34) (2010) 11110–11116, https://doi.org/10.1021/jp103292e.

[60] M. Mecke, J. Winkelmann, J. Fischer, Molecular dynamics simulation of the liquid-vapor interface: binary mixtures of Lennard-Jones fluids, J. Chem. Phys. 110 (2) (1999) 1188–1194, https://doi.org/10.1063/1.478160.

[61] V.G. Baidakov, S.P. Protsenko, Molecular-dynamics investigation of phase equilibrium and surface tension in argon-neon system, J. Phys. Chem. C 112 (44) (2008) 17231–17234, https://doi.org/10.1021/jp805566g.

[62] L.M. Pereira, A. Chapoy, R. Burgass, B. Tohidi, Measurement and modelling of high pressure density and interfacial tension of (gas + n-alkane) binary mixtures, J. Chem. Thermodyn. 97 (2016) 55–69, https://doi.org/10.1016/j.jct.2015.12.036.

[63] J. Algaba, M. Cartes, M. A, J.M. Miguez, F.J. Blas, Phase equilibria and interfacial properties of the tetrahydrofuran + methane binary mixture from experiment and computer simulation, J. Phys. Chem. C 123 (34) (2019) 20960–20970, https://doi.org/10.1021/acs.jpcc.9b05412.

[64] N. Choudhary, A.K. Nair, M.F. Ruslan, S. Sun, Bulk and interfacial properties of decane in the presence of carbon dioxide, methane, and their mixture, Sci. Rep. 9 (1) (2019) 1–10, https://doi.org/10.1038/s41598-019-56378-y.

[65] P.I.C. Teixeira, B.S. Almeida, M.M. Telo da Gama, J.A. Rueda, R.G. Rubio, Interfacial properties of mixtures of molecular fluids: comparison between theory and experiment; methyl iodide + carbon tetrachloride and acetonitrile + carbon tetrachloride, J. Phys. Chem. 96 (21) (1992) 8488–8497, https://doi.org/10.1021/j100200a053.

[66] J. Aracil, G. Luengo, B.S. Almeida, M.M. Telo da Gama, R.G. Rubio, M. Diaz Pena, Surface properties of mixtures of molecular fluids: an experimental and theoretical study of carbon disulfide + dichloromethane and carbon disulfide + carbon tetrachloride, J. Phys. Chem. 93 (8) (1989) 3210–3218, https://doi.org/10.1021/j100345a065.

[67] S.P. Protsenko, V.G. Baidakov, Binary Lennard-Jones mixtures with highly asymmetric interactions of the components. 1. effect of the energy parameters on phase equilibria and properties of liquid-gas interfaces, Fluid Phase Equilib. 429 (2016) 242–253, https://doi.org/10.1016/j.fluid.2016.09.009.

[68] E. Salomons, M. Mareschal, Surface tension, adsorption and surface entropy of liquid-vapour systems by atomistic simulation, J. Phys. Condens. Matter 3 (20) (1991) 3645–3661, https://doi.org/10.1088/0953-8984/3/20/025.

[69] B. Ibarra-Tandi, A. Lira, J. Lopez-Lemus, Effect of softness on relative adsorption for binary mixtures of simple fluids, J. Mol. Liq. 185 (2013) 62–69, https://doi.org/10.1016/j.molliq.2012.12.004.

[70] O.G. Niño-Amézquita, D. van Putten, S. Enders, Phase equilibrium and interfacial properties of water+CO_2 mixtures, Fluid Phase Equilibria 332 (2012) 40, https://doi.org/10.1016/j.fluid.2012.06.018.

[71] F.J. Martinez-Ruiz, F.J. Blas, Interfacial properties of binary mixtures of square-well molecules from Monte Carlo simulation, J. Chem. Phys. 144 (15) (2016) 154705, https://doi.org/10.1063/1.4947017.

[72] O.G. Niño-Amézquita, S. Enders, P.T. Jaeger, R. Eggers, Measurement and prediction of interfacial tension of binary mixtures, Ind. Eng. Chem. Res. 49 (2) (2010) 592–601, https://doi.org/10.1021/ie901209z.

[73] W. Li, Z. Jin, Molecular dynamics simulation of natural gas-water interfacial tensions over wide range of pressures, Fuel 236 (2019) 480–492, https://doi.org/10.1016/j.fuel.2018.09.040.

[74] P. Ungerer, D. Rigby, B. Leblanc, M. Yiannourakou, Sensitivity of the aggregation behaviour of asphaltenes to molecular weight and structure using molecular dynamics, Mol. Simul. 40 (1–3) (2014) 115–122, https://doi.org/10.1080/08927022.2013.850499.

[75] T.F. Headen, E.S. Boek, N.T. Skipper, Evidence for asphaltene nanoaggregation in toluene and heptane from molecular dynamics simulations, Energy & Fuels 23 (3) (2009) 1220–1229, https://doi.org/10.1021/ef800872g.

[76] S. Plimpton, Fast parallel algorithms for short-range molecular dynamics, J. Comp. Phys. 117 (1995) 1–19.

[77] J. Gross, G. Sadowski, Perturbed-Chain SAFT: An equation of state based on a perturbation theory for chain molecules, Ind. Eng. Chem. Res. 40 (4) (2001) 1244, https://doi.org/10.1021/ie0003887.

[78] G.M. Kontogeorgis, E.C. Voutsas, I.V. Yakoumis, D.P. Tassios, An equation of state for associating fluids, Ind. Eng. Chem. Res. 35 (11) (1996) 4310–4318, https://doi.org/10.1021/ie9600203.

[79] T. Lafitte, A. Apostolakou, C. Avendaño, A. Galindo, C.S. Adjiman, E.A. Müller, G. Jackson, Accurate statistical associating fluid theory for chain molecules formed from Mie segments, J. Chem. Phys. 139 (15) (2013) 154504, https://doi.org/10.1063/1.4819786.

[80] G.M. Kontogeorgis, M.L. Michelsen, G.K. Folas, S. Derawi, N. von Solms, E.H. Stenby, Ten years with the CPA (cubic-plus-association) equation of state. part 1. pure compounds and self-associating systems 45(14) 4855–4868. 10.1021/ie051305v.

[81] J. Gross, G. Sadowski, Application of the perturbed-chain SAFT equation of state to associating systems, Ind. Eng. Chem. Res. 41 (22) (2002) 5510–5515, https://doi.org/10.1021/ie010954d.

[82] S. Dufal, T. Lafitte, A. Galindo, G. Jackson, A.J. Haslam, Developing intermolecular-potential models for use with the SAFT-VR Mie equation of state, AIChE Journal 61 (9) (2015) 2891–2912, https://doi.org/10.1002/aic.14808.

[83] X. Mu, F. Frank, F.O. Alpak, W.G. Chapman, Stabilized density gradient theory algorithm for modeling interfacial properties of pure and mixed systems, Fluid Phase Equilib. 435 (2017) 118–130, https://doi.org/10.1016/j.fluid.2016.11.024.

[84] Y.M. Muñoz-Muñoz, G. Guevara-Carrion, J. Vrabec, Molecular insight into the liquid propan-2-ol + water mixture, J. Phys. Chem. B 122 (37) (2018) 8718–8729, https://doi.org/10.1021/acs.jpcb.8b05610.

[85] R. Li, C. D'Agostino, J. McGregor, M.D. Mantle, J.A. Zeitler, L.F. Gladden, Mesoscopic structuring and dynamics of alcohol/water solutions probed by terahertz time-domain spectroscopy and pulsed field gradient nuclear magnetic resonance, J. Phys. Chem. B 118 (34) (2014) 10156–10166, https://doi.org/10.1021/jp502799x.

[86] S. Choi, S. Parameswaran, J.-H. Choi, Effects of molecular shape on alcohol aggregation and water hydrogen bond network behavior in butanol isomer solutions, Phys. Chem. Chem. Phys. 23 (2021) 12976–12987, https://doi.org/10.1039/D1CP00634G.

[87] I.A. McLure, B. Edmonds, M. Lal, Extremes in surface tension of fluorocarbon + hydrocarbon mixtures, Nature Physical Science 241 (107) (1973), https://doi.org/10.1038/physci241071a0.71–71

[88] W.A. Fouad, L.F. Vega, The phase and interfacial properties of azeotropic refrigerants: the prediction of aneotropes from molecular theory, Phys. Chem. Chem. Phys. 19 (2017) 8977–8988, https://doi.org/10.1039/C6CP08031F.

[89] Dortmund data bank (accessed January 2022), 2022, (www.ddbst.com).

[90] J. Lekner, J.R. Henderson, Surface tension and energy of a classical liquid-vapour interface, Mol. Phys. 34 (2) (1977) 333–359, https://doi.org/10.1080/00268977700101771.